SCIENCE CHINA
Information Sciences

• LETTER •

May 2026, Vol. 69, Iss. 5, 159402:1–159402:2
https://doi.org/10.1007/s11432-025-4616-7

High threshold voltage and enhanced threshold voltage stability of Schottky p-GaN gate HEMT by p-GaN bridge engineering

Kuo ZHANG, Kai LIU, Yunlong HE, Chong WANG*, Wentao ZHANG, Xuefeng ZHENG, Xiaohua MA & Yue HAO

Key Laboratory of Wide Bandgap Semiconductor Technology, School of Microelectronics, Xidian University, Xi'an 710071, China

Received 15 January 2025/Revised 15 April 2025/Accepted 29 September 2025/Published online 1 April 2026

Citation Zhang K, Liu K, He Y L, et al. High threshold voltage and enhanced threshold voltage stability of Schottky p-GaN gate HEMT by p-GaN bridge engineering. Sci China Inf Sci, 2026, 69(5): 159402, https://doi.org/10.1007/s11432-025-4616-7

Enhancement-mode p-GaN gate HEMTs are well-suited for power electronics applications due to their balanced electrical performance and manufacturing stability [1]. In particular, Schottky-type p-GaN gate offers reduced gate leakage and enhanced gate operating voltage. However, Schottky p-GaN HEMTs still face key challenges such as low threshold voltage ($V_{\rm TH}$) and significant $V_{\rm TH}$ instability under both gate and drain bias stress [2, 3]. The source-connected p-GaN HEMT has been proposed as an effective approach for enhancing $V_{\rm TH}$ [4]. Subsequently, p-GaN bridges are implemented in AlGaN-channel ohmic-type p-GaN gate HEMTs [5], achieving higher $V_{\rm TH}$ but with significant gate leakage. However, the physical mechanisms through which the p-GaN bridge enhances $V_{\rm TH}$ remain inadequately understood and require deeper investigation. More importantly, the integration of multiple p-GaN bridges into Schottky p-GaN HEMTs and their potential advantages for enhancing $V_{\rm TH}$ and $V_{\rm TH}$ stability remains largely unexplored and warrants further comprehensive investigation.

In this work, we propose the integration of multiple p-GaN bridges into Schottky-type p-GaN gate HEMTs (PB-HEMTs), achieving significant threshold voltage ($V_{\rm TH}$) enhancement and enabling wide-range $V_{\rm TH}$ modulation by varying the number of bridges. To elucidate the $V_{\rm TH}$ enhancement mechanism, a gate equivalent circuit model is developed and comprehensively analyzed. Importantly, it is demonstrated that the multiple p-GaN bridges structure effectively functions as the discharge path for the floating p-GaN layer, substantially improving $V_{\rm TH}$ stability under gate and drain voltage stress. Moreover, the gate metal/p-GaN Schottky junction continues to function, thereby ensuring low gate leakage.

Experiment. Figures 1(a) and (b) illustrate the structure and micrograph of the PB-HEMT. Details of the device fabrication process can be found in Appendix A.

Results and discussion. Figure 1(c) shows the transfer characteristics of the C-HEMT and PB-HEMTs with 1, 2, 3, 4, and 5 bridges. The PB-HEMTs demonstrate a significantly enhanced $V_{\rm TH}$, with a wide modulation range from 2.25 to 3.05 V achievable by varying the number of p-GaN bridges. The on-resistance of the PB-HEMT exhibits a slight increase with a greater number of bridges (Figure 1(d)). As shown in Figure 1(e), the PB-HEMTs exhibit a slight increase in gate forward leakage ($I_{\rm G}$) compared to the C-HEMT, which is attributed to additional gate-to-source leakage paths introduced by the p-GaN bridges. Nevertheless, the reverse-biased metal/p-GaN Schottky junction in PB-HEMT remains functional, thereby maintaining the $I_{\rm G}$ at a low level. The transfer length method (TLM) measurements of the p-GaN/source ohmic contact characteristics indicate relatively high current and a low reverse barrier, suggesting that the p-GaN/source metal contact forms a weak Schottky junction with high leakage ($J_{\rm HL\text{-}SCH}$) as shown in Figure 1(f). Therefore, the p-GaN bridges are sufficient to establish conductive paths for charge transfer between the gate and source before the channel is fully turned on.

Figures 1(g)–(i) show the equivalent gate circuits of C-HEMT and PB-HEMT. The gate stack of the C-HEMT can be modelled as a p-GaN/metal Schottky junction ($J_{\rm SCH}$) with a p-GaN/AlGaN/GaN PIN junction ($J_{\rm PIN}$) connected back-to-back in series [3]. In the PB-HEMT, the $J_{\rm HL\text{-}SCH}$ and the p-GaN bridge resistance create a secondary path in parallel with $J_{\rm PIN}$ between the gate and source. The source ground potential is transmitted through this path into the p-GaN, thereby reducing the electrical potential ($V_{\rm PIN}$) at the anode of $J_{\rm PIN}$ diode. Consequently, PB-HEMT requires a higher gate voltage to elevate $V_{\rm PIN}$ to the level necessary for channel turn-on, resulting in an increased $V_{\rm TH}$.

To comprehensively evaluate the $V_{\rm TH}$ stability of both the C-HEMT and PB-HEMTs, dynamic and static bias stress tests have been conducted respectively. Figure 1(j) demonstrates that under 0–40 V pulsed drain stress, the C-HEMT exhibits a substantial positive $V_{\rm TH}$ shift of 0.78 V, while the PB-HEMT shows a significantly reduced shift of only 0.21 V. More notably, under pulsed gate stress (Figure 1(k)), the PB-HEMT maintains exceptional stability with a negligible $V_{\rm TH}$ shift of merely 0.09 V, in sharp contrast to the considerable negative shift of 0.92 V observed in the C-HEMT. The superior $V_{\rm TH}$ stability of the PB-HEMT is further demonstrated under static bias conditions (Figures 1(l)

* Corresponding author (email: chongw@xidian.edu.cn)

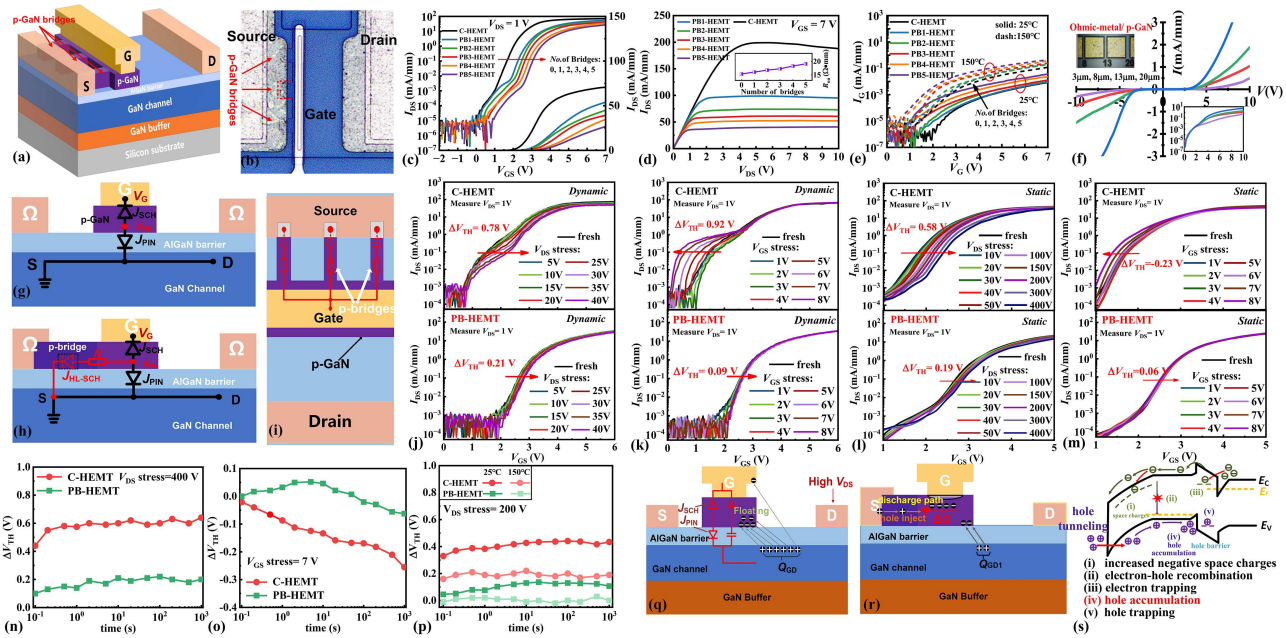

Figure 1 (Color online) (a) Schematic diagram and (b) micrograph of PB-HEMT; (c) transfer (d) output (e) gate leakage characteristics of C-HEMT and PB-HEMT with 1, 2, 3, 4, and 5 bridges; (f) TLM test results of p-GaN/source ohmic contact; equivalent gate circuits of (g) C-HEMT and (h) PB-HEMT; (i) top view of equivalent circuit the PB-HEMT with three bridges; transfer curves of C-HEMT and PB-HEMT (with three bridges) under (j) pulsed drain stress, (k) pulsed gate stress, (l) static drain stress, (m) static gate stress; V_{TH} shifts of two devices under long-term stress: (n) V_{DS} = 400 V, (o) V_{GS} = 7 V, and (p) V_{DS} = 200 V at 25°C and 150°C; (q) charge storage mechanism in p-GaN under high drain stress; (r) charge release mechanism through the p-GaN bridges of PB-HEMT; (s) band diagrams of Schottky p-GaN HEMT gate region under forward gate bias stress.

and (m)). The PB-HEMT exhibits remarkably small V_{TH} shifts of 0.19 V under 400 V drain stress and 0.06 V under 8 V gate stress, representing a substantial improvement over the C-HEMT. The V_{TH} stability of PB-HEMTs with 1 to 5 bridges is systematically characterized. As the p-GaN bridge count increases, the drain-induced V_{TH} shift decreases monotonically. Meanwhile, the gate-induced V_{TH} shift exhibits a negative reduction followed by a positive increase, primarily attributed to the competition between positive and negative charge storage. Detailed results and discussions are provided in Appendixes D and E. Figures 1(n) and (o) demonstrate the superior V_{TH} stability of PB-HEMT compared to C-HEMT under long-term (0–1000 s) bias stress at V_{DS} = 400 V and V_{GS} = 7 V, respectively. Furthermore, PB-HEMT maintains stable V_{TH} under high-temperature stress at 150°C, as shown in Figure 1(p).

The V_{TH} instability in Schottky p-GaN gate HEMTs is primarily attributed to the storage of non-equilibrium charges in the p-GaN layer [2]. Under high drain stress, hole emission from the p-GaN layer toward the gate occurs, resulting in hole deficiency in p-GaN layer (Figure 1(q)). When switched to the on-state, the reverse-biased J_{SCH} under forward gate bias inhibits hole replenishment, while the resulting accumulation of negative charges in p-GaN layer induces a positive V_{TH} shift. Conversely, under high gate stress (Figure 1(s)), excessive hole injection into p-GaN layer leads to positive charge accumulation, causing negative V_{TH} shifts. In PB-HEMT, the unique multi-bridge structure enables rapid hole transfer to the floating p-GaN through the source connection, effectively releasing the non-equilibrium negative charges accumulated in p-GaN layer after drain stress (Figure 1(r)). By the same mechanism, the excessive hole injection and accumulation in p-GaN layer under forward gate stress can be efficiently released through the p-GaN bridges to source electrode. Consequently, the PB-HEMT demonstrates exceptional V_{TH} stability under both high drain and gate bias stress.

Conclusion. We propose to increase the V_{TH} and enhance the V_{TH} stability of Schottky p-GaN gate HEMTs through multiple p-GaN bridges engineering. By varying the number of p-GaN bridges, a wide range of V_{TH} modulation can be achieved. The enhanced V_{TH} stability is attributed to the role of the p-GaN bridges as discharge paths for the floating p-GaN layer, which facilitates rapid charge release and replenishment, thereby effectively suppressing the charge storage effect. The fabrication of the PB-HEMT is compatible with conventional p-GaN gate HEMT processes without requiring additional steps, indicating strong potential for highly reliable power electronics applications.

Acknowledgements This work was supported by National Natural Science Foundation of China (Grant No. 62188102).

Supporting information Appendixes A–E. The supporting information is available online at info.scichina.com and link.springer.com. The supporting materials are published as submitted, without typesetting or editing. The responsibility for scientific accuracy and content remains entirely with the authors.

References

1 Wei J, Zheng Z, Tang G, et al. GaN power integration technology and its future prospects. IEEE Trans Electron Device, 2024, 71: 1365–1382
2 Wei J, Xie R, Xu H, et al. Charge storage mechanism of drain induced dynamic threshold voltage shift in p-GaN gate HEMTs. IEEE Electron Device Lett, 2019, 40: 526–529
3 Sayadi L, Iannaccone G, Sicre S, et al. Threshold voltage instability in p-GaN gate AlGaN/GaN HFETs. IEEE Trans Electron Device, 2018, 65: 2454–2460
4 Hwang I, Oh J, Choi H S, et al. Source-connected p-GaN gate HEMTs for increased threshold voltage. IEEE Electron Device Lett, 2013, 34: 605–607
5 Zhang L, Zhou H, Zhang W, et al. AlGaN-channel gate injection transistor on silicon substrate with adjustable 4–7-V threshold voltage and 1.3-kV breakdown voltage. IEEE Electron Device Lett, 2018, 39: 1026–1029